Solid-State Electronics 101 (2014) 116–121

Contents lists available at ScienceDirect

Solid-State Electronics

journal homepage: www.elsevier.com/locate/sse

Spin injection in a semiconductor through a space-charge layer

Joydeep Ghosh *, Thomas Windbacher, Viktor Sverdlov, Siegfried Selberherr

Institute for Microelectronics, TU Wien, Gußhausstraße 27-29, A-1040 Wien, Austria

ARTICLE INFO

Article history:
Available online 14 July 2014

The review of this paper was arranged by Prof. A. Zaslavsky.

Keywords:
Spin transport
Spin injection
Space-charge layer
Spin threshold current

ABSTRACT

The electron spin properties provided by semiconductors are of immense interest because of their potential for future spin-driven microelectronic devices. Modern charge-based electronics is dominated by silicon, and understanding the details of spin propagation in silicon structures is key for novel spin-based device applications. We performed simulations on electron spin transport in an n-doped silicon bar with spin-dependent conductivity. Special attention is paid to the investigation of a possible spin injection enhancement through an interface space-charge layer. We found substantial spin transport differences between the spin injection behavior through an accumulation and a depletion layer. However, in both cases the spin current density can not be significantly higher than the spin current density at charge neutrality. Thus, the maximum spin current in the bulk is determined by its value at the charge neutrality condition - provided the spin polarization at the interface as well as the charge current are fixed.

1. Introduction

The tremendous increase of computational power of integrated circuits is supported by the continuing miniaturization of semiconductor devices' feature size. However, with scaling approaching its fundamental limits the semiconductor industry is facing the necessity for new engineering solutions and innovative techniques to improve MOSFET performance. Spin-based electronics (spintronics) is a promising successor technology which facilitates the use of spin as a degree of freedom to reduce the device power consumption [1,2]. Moreover, the spintronic devices are expected to be faster and more compact.

Silicon, the main material of microelectronics, possesses several properties attractive for spintronics [3]: it is composed of nuclei with predominantly zero spin and it is characterized by weak spin–orbit interaction, which should result in a low relaxation rate accompanied by a longer spin lifetime as compared to other semiconductors. Since silicon technology is well established, it will help bringing silicon spin-driven devices to the market. Spin transfer in silicon over long distances has been demonstrated experimentally [4], and a large number of devices utilizing spin has already been proposed [5].

Regardless of the indisputable advantage in realizing spin injection, detection, and the spin transport in silicon at ambient temperature, several difficulties not explained within the theories are pending. One of them is an unrealistically high amplitude of the voltage signal corresponding to the spin accumulation in silicon obtained within the three-terminal spin injection/detection scheme [3]. Recently, an explanation based on the assumption that the resonant tunneling magnetoresistance effect and not the spin accumulation causes the electrically dependent spin signal in local three-terminal detection experiments, was proposed [6,7]. It remains to be seen, if the theory is able to explain all the data including the spin injection experiments through a single graphene layer, where the amplitude of the signal is consistent with the spin accumulation in silicon [8]. Alternatively, an evidence that a proper account of space-charge effects at the interface may boost the spin injection signal by an order of magnitude was presented [9].

In this paper we investigate the influence of the space-charge effects to boost spin injection in semiconductors. Considering charge accumulation and depletion at the spin injection boundary, we observe major differences in the spin current behavior. The existence of the upper threshold spin current under high spin accumulation [10] is confirmed. We demonstrate that the threshold spin current in the bulk is determined by the spin current value injected at the charge neutrality condition under the assumption that the spin polarization and the charge current are fixed. We show that in accumulation the ratio of the spin density s to the charge concentration n, or the spin polarization $P = s/n$, remains

* Corresponding author. Tel.: +43 15880136060.
E-mail addresses: ghosh@iue.tuwien.ac.at (J. Ghosh), windbacher@iue.tuwien.ac.at (T. Windbacher), sverdlov@iue.tuwien.ac.at (V. Sverdlov), selberherr@iue.tuwien.ac.at (S. Selberherr).

http://dx.doi.org/10.1016/j.sse.2014.06.035
0038-1101/

practically unchanged due to the narrow accumulation layer. Therefore, the spin and the spin current densities decay fast through the accumulation layer determined by the decrease of the charge concentration from its high value at the interface to the equilibrium value determined by the bulk donor concentration. The spin current in the bulk is determined by the spin polarization and the charge current density at the end of the accumulation layer, where the charge neutrality condition is fulfilled. In depletion, however, the situation can be more complex. In the case when the spin diffusion is against the electric field, the spin current remains constant through the depletion region. But, due to the large influx of the minority spins into the depletion layer the spin polarization decreases drastically which causes a significant reduction of the spin current in the bulk as compared to that at the charge neutrality condition. Thus, in both cases of spin transport through the depletion and accumulation region the spin current density cannot be significantly higher than the spin current density at the charge neutrality condition, the value of which is determined by the spin polarization at the interface and the value of the electric field.

We begin with a short review of the spin and charge drift–diffusion equations in the next section. In contrast to the highly nonlinear set of equations describing the transport in the language of chemical potentials [10] suitable for metals, we use the employed equations to describe the transport properties in semiconductors [11,12]. Due to its importance, the solution at the charge neutrality condition is presented next. The system of equations for the electrostatic potential, charge density, spin density, and currents are solved numerically to investigate the spin injection in depletion and accumulation. The boundary conditions used to introduce the non-equilibrium charge density at the interface and thus a nonzero total charge in the system distinguish our approach from the one employed in [12]. The analytical solution at the charge-neutrality condition is used in order to validate the numerical solution. Finally, a discussion of the numerical results is presented.

2. Model

The spin drift–diffusion model is successfully used to describe the classical transport of charge carriers and their spins in a semiconductor. The expression for up (down)-spin current, $J_{\uparrow(\downarrow)}$, can be written as [11]:

$$J_{\uparrow(\downarrow)} = en_{\uparrow(\downarrow)}\mu E + eD\nabla n_{\uparrow(\downarrow)}, \tag{1}$$

where D is the electron diffusion coefficient, μ is the electron mobility, E denotes the electric field, and e is the absolute charge of an electron. The up (down)-spin concentration is expressed as $n_{\uparrow}(n_{\downarrow})$. The electron concentration is thus represented as $n = n_{\uparrow} + n_{\downarrow}$ and the spin density $s = n_{\uparrow} - n_{\downarrow}$. The electron (spin) current is defined as [11] $J_n(J_s) = J_{\uparrow} \pm J_{\downarrow}$.

The steady-state continuity equation for the up (down)-spin electrons including the spin scattering reveals [11]:

$$\nabla \cdot J_{\uparrow(\downarrow)} = \pm e\left(\frac{n_{\uparrow} - n_{\downarrow}}{\tau}\right), \tag{2}$$

where $\tau_s = \frac{\tau}{2}$ is the spin relaxation time. The Poisson equation, defining the electric field, reads:

$$\nabla \cdot E = -e\frac{n_{\uparrow} + n_{\downarrow} - N_D}{\epsilon_{Si}}, \tag{3}$$

where ϵ_{Si} is the electric permittivity of silicon and N_D is the doping concentration. We denote V_{th} as the thermal voltage: $V_{th} = \frac{K_B T}{q}$, where K_B is the Boltzmann constant, T the temperature ($T = 300$ K), $q = e$. The intrinsic spin diffusion length is defined as $L = \sqrt{D\tau_s}$ and the diffusion coefficient D is related to the mobility by the Einstein relation $D = \mu V_{th}$. The charge current and the spin currents are:

$$J_n = en\mu E + eD\frac{dn}{dx}, \tag{4}$$

$$J_s = es\mu E + eD\frac{ds}{dx}. \tag{5}$$

The spin density affirms:

$$\frac{d^2 s}{dx^2} + \left(\frac{1}{V_{th}}\right)\frac{d(sE)}{dx} - \frac{s}{L^2} = 0, \tag{6}$$

where both s and E are position dependent. The spin drift–diffusion equation must be solved self-consistently with the Poisson and charge transport equation.

2.1. Spin injection at charge neutrality

Eq. (6) as well as the charge drift–diffusion equation and the Poisson equation must be supplemented with appropriate boundary conditions. We consider charge and spin transport through a bar of length W. We assume that the spin density is zero at the right interface while the charge concentration is equal to N_D:

$$s(x = W) = n_{\uparrow}^{W} - n_{\downarrow}^{W} = 0,$$
$$n(x = W) = n_{\uparrow}^{W} + n_{\downarrow}^{W} = N_D.$$

Here, $n_{\uparrow(\downarrow)}^{w}$ is the up (down)-spin concentration at the right contact.

At the left boundary the spin value is kept constant:

$$s(x = 0) = s^0 = n_{\uparrow}^0 - n_{\downarrow}^0. \tag{7}$$

Here, $n_{\uparrow(\downarrow)}^0$ is the up (down)-spin concentration at the spin injection point. The electron concentration n^0 at the interface is defined by:

$$n(x = 0) = n_{\uparrow}^0 + n_{\downarrow}^0 = n^0. \tag{8}$$

These boundary conditions are different from the von Neumann boundary conditions used in [10] and allow to describe the spin current not only for an accumulation layer but also for a depletion layer. The set of the boundary conditions must be supplemented by defining the electrostatic potential difference U_c between the left and right boundary of the semiconductor bar, which defines the electrostatic field obtained by the Poisson equation.

By this, the same spin density value s^0 at the interface can be provided for different n^0. Therefore, the total charge at the interface n^0 offers an additional degree of freedom and allows to study the influence of the space-charge layer at the interface on the efficiency of the spin injection and transport in a semiconductor. If we affix $n^0 = N_D$, the charge neutrality at the interface (and as a consequence throughout the whole sample) is preserved. In this case, the electric field E will be constant throughout the bar and the expression for the electron charge current (4) is $J_c = eN_D\mu E$, where E is defined by the applied voltage and W as $E = U_c/W$. The general solution for the spin density is [11,10]:

$$s = A_1 \exp\left(\frac{-x}{L_d}\right) + A_2 \exp\left(\frac{x}{L_u}\right). \tag{9}$$

The constants A_1 and A_2 are defined by the boundary conditions. Here, the electric field dependent up (down)-spin diffusion length is given by:

$$L_u(L_d) = \frac{1}{\pm\frac{|eE|}{2K_B T} + \sqrt{\left(\frac{eE}{2K_B T}\right)^2 + \frac{1}{L^2}}}. \tag{10}$$

Therefore, $L_u(L_d)$ monotonically decreases (increases) with the applied electric field and its direction.

For fixing the spin concentration s^0 at the left boundary, one obtains:

$$A_{1(2)} = \pm s^0 \frac{\exp\left(\frac{\pm W}{L_{u(d)}}\right)}{\exp\left(\frac{W}{L_u}\right) - \exp\left(\frac{-W}{L_d}\right)}. \quad (11)$$

The corresponding expression for the spin current reads as:

$$J_s = q\mu E\left[\left(1 + \frac{V_{th}}{EL_u}\right)A_2 \exp\left(\frac{x}{L_u}\right) + \left(1 - \frac{V_{th}}{EL_d}\right)A_1 \exp\left(\frac{-x}{L_d}\right)\right]. \quad (12)$$

We used the analytical results to check our simulation framework, which was later used to study the spin injection through a space-charge layer. Under the charge neutrality condition, a good agreement between the numerically simulated results and the analytical expressions are obtained for the spin density (Fig. 1) for several values of the applied voltage U_c. The presence of the electric field modifies $L_u(L_d)$ (cf. (10)) and hence the spin density. A comparison of the simulated spin current density to (12) is shown in Fig. 2.

In Fig. 3, we show the variation of the spin current for different boundary spin polarizations under the charge neutrality condition (*CN*). No voltage is applied, hence, the charge current is absent. The spin current through the bar monotonically increases with the spin polarization P^0, reaching its maximum when P^0 is maximum (i.e. $P^0 = 1$). This is in agreement with the results from [10]. One has to note that although the spin polarization is 100% at $P^0 = 1$, we do not observe any enhancement of the spin diffusion length as predicted in [10]. Even at $P^0 = 1$, and at the charge neutrality condition where the spin is completely decoupled from charge, the spin diffusion length is only determined by the intrinsic spin diffusion length L and the value and the direction of the electric field E as it follows from (10).

In the following we study spin injection in the presence of space-charge effects, when analytical results are not available.

2.2. Spin injection through the space-charge layer

In a semiconductor the up (down)-spin chemical potential is related to its concentration via [11]:

$$\mu_{\uparrow(\downarrow)} = V_{th} \ln \frac{n_{\uparrow(\downarrow)}}{n^{eql}_{\uparrow(\downarrow)}}. \quad (13)$$

$n^{eql}_{\uparrow(\downarrow)}$ represents up (down)-spin concentration at equilibrium ($0.5N_D$ for silicon).

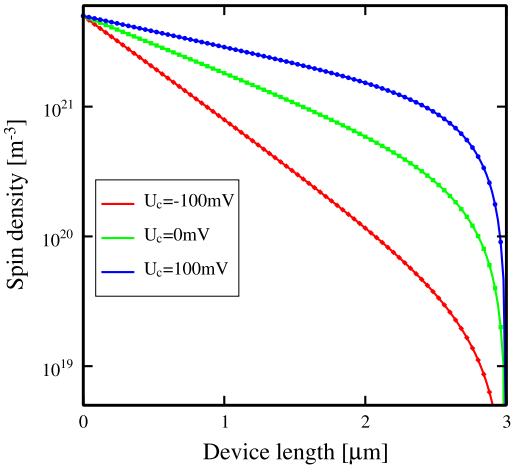

Fig. 1. Comparison of the spin density between the numerically simulated results and the analytical expression (9) under charge neutrality. The spin polarization $P = 0.5$ is fixed at the left boundary (Lines→ Theory, Dots → Simulation).

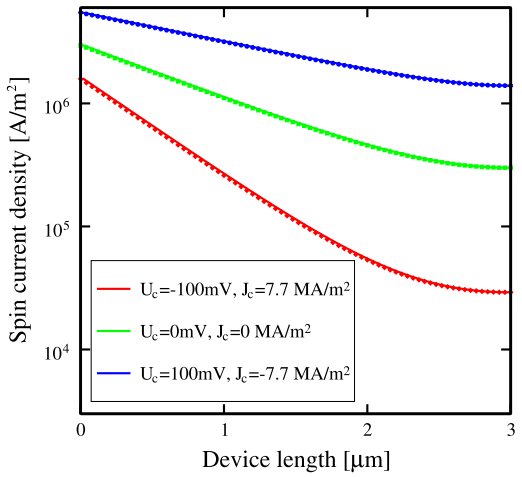

Fig. 2. Comparison of the spin current density between the numerically simulated results and the analytical expression (12) under charge neutrality, corresponding to Fig. 1 (Lines→ Theory, Dots → Simulation).

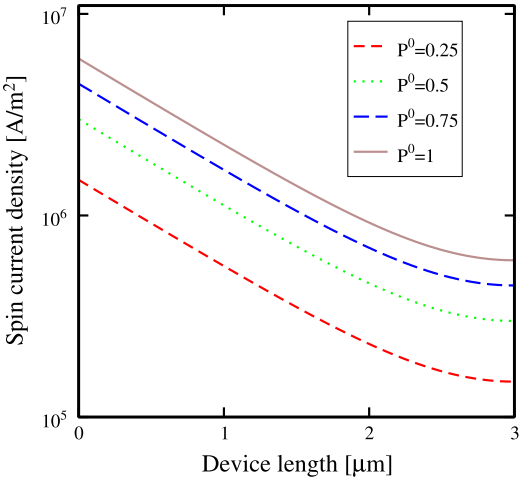

Fig. 3. Spin current density depending upon the boundary spin polarization (P^0) and under charge neutrality condition. The charge current is kept zero.

To study the effects of the space-charge layer on spin transport we consider the maximal spin polarization $P^0 = s^0/n^0 = 1$ at the injection boundary. In this case the spin and charge density at the interface can be fixed through the single parameter $\mu_{Chem} = V_{th} \ln(s^0/N_D)$. The spin polarization at the left boundary is kept maximal through the following boundary condition for up (down) concentrations:

$$\begin{bmatrix} n^0_{\uparrow} \\ n^0_{\downarrow} \end{bmatrix} = N_D \begin{bmatrix} \exp\left(\frac{\mu_{Chem}}{V_{th}}\right) \\ 0 \end{bmatrix}. \quad (14)$$

Here, μ_{Chem} defines the charge chemical potential. We can inject (release) up-spin and hence the charge at the same time. We therefore can describe:

- spin injection at charge neutrality ($\mu_{Chem} = 0$),
- spin injection at charge accumulation ($\mu_{Chem} > 0$),
- spin injection at charge depletion ($\mu_{Chem} < 0$).

Simulations were performed by the finite volume method (FVM) [13] for an *n*-semiconductor bar with an intrinsic spin diffusion length of L = 1 μm. A bar length of several microns, a doping concentration of $N_D = 10^{16}\,\mathrm{cm}^{-3}$, and an electron mobility of 1400 $\mathrm{cm}^2\,\mathrm{V}^{-1}\,\mathrm{s}^{-1}$ were assumed, and a voltage U_c is applied.

3. Results and discussion

Via (14) a considerable spin and charge accumulation (depletion) at the interface can be introduced and hence a spin current can diffuse out of this region. The spin and the charge current through the bar can be tuned by varying the chemical potential and the applied voltage. Charge injection or charge release always cause a non-zero charge current in the device, even at the absence of an external electric field. This charge current can be compensated by applying an external voltage, given by the equation:

$$U_c = -V_{th} \ln\left(\frac{n_\uparrow^0 + n_\downarrow^0}{N_D}\right). \tag{15}$$

3.1. Accumulation: spin current saturation

First, we investigate the carrier distribution and current variation along the bar considering charge accumulation and a fixed charge current. The charge current density in the bar has been set to 11.9 MA/m^2. The dependence of the charge current density on the chemical potential (μ_{Chem}) at varied electric field is depicted in Fig. 4. The voltage applied has to be adjusted in order to keep the current density constant. Strong nonlinear effects due to the conductivity variation in the space-charge layer close to the left boundary cause deviations of the compensating voltage from (15), when the bar moves from accumulation to deep depletion. An abundance of spin carriers during the accumulation enhances the spin current close to the interface, while a lack of spin carriers in depletion causes a very strong diminution of the spin current. Fig. 5 reveals that under charge accumulation, the spin current shows an upper threshold [10]. The amount of the spin current which leaks from the accumulation region almost does not change in high accumulation, regardless of the high value of spin density and spin current at the interface. This means that an effort to boost the spin current by increasing the spin concentration at the interface to inject more spin polarized electrons does not result in a substantial spin current increase [10].

In order to further investigate the spin current enhancement (at the boundaries or in the bulk) due to a charge accumulation, we show the variation of the spin current for different boundary spin polarizations. Fig. 6 reveals that for $P^0 = 1$ the spin current close to the spin injection interface is significantly higher at charge accumulation compared to that at *CN*. However, at a distance of about λ_D from the interface, the spin current becomes similar to that at the interface under *CN* and the same spin polarization. If $P^0 < 1$, our results indicate that it is not possible to obtain a spin current in the bulk as high as for $P^0 = 1$, even under higher charge accumulation at the interface, and the current is close to that under the charge neutrality condition with the same P^0.

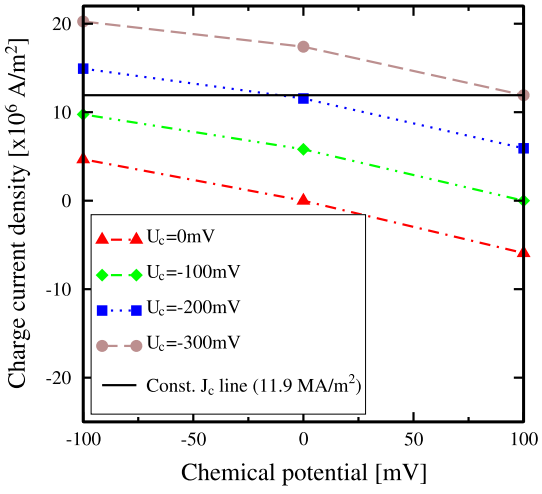

Fig. 4. The variation of the charge current density (J_c) as a function of the chemical potential defined by (14) and the external voltage (U_c). One extra line also indicates a constant J_c. The device length is 4 μm.

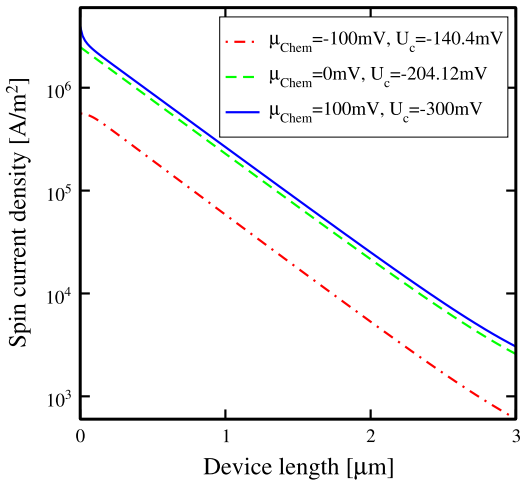

Fig. 5. Variation of the spin current density under boundary condition (14), depicting the presence of an upper saturation at charge accumulation. Charge current is fixed to 11.9 MA/m^2.

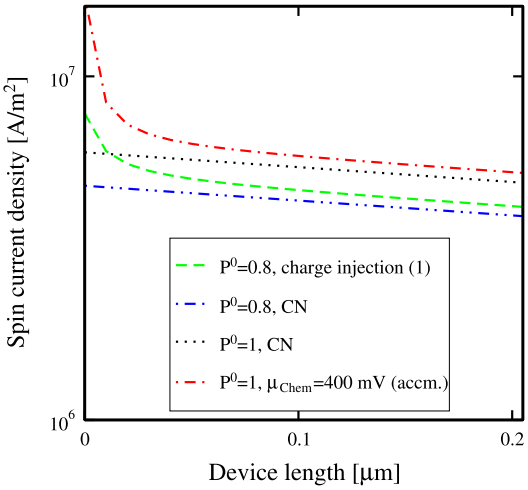

Fig. 6. Spin current density for up to 5 times the Debye length λ_D from the left boundary under charge neutrality (*CN*) and charge accumulation. The charge current is zero. The left boundary for (1) is set with $n^0 = 1000N_D$.

In order to explain this behavior we plot the spin polarization, the charge, and the spin density close to the interface (Fig. 7). The spin polarization remains approximately constant through the accumulation layer, while the charge decrease from its high value at the interface to the equilibrium value is determined by the doping concentration N_D. Therefore, the spin density also decreases substantially. Thus, the spin current in the bulk is determined by the spin density at the end of the accumulation layer, where the charge neutrality condition is restored and is thus determined by the spin current density at the charge neutrality condition with the same spin polarization.

3.2. Depletion: spin current reduction

At depletion, when the spin diffusion is along the current, we observe a substantial decrease of the spin and the spin current densities, both at the interface and the bulk (Fig. 8) as compared to

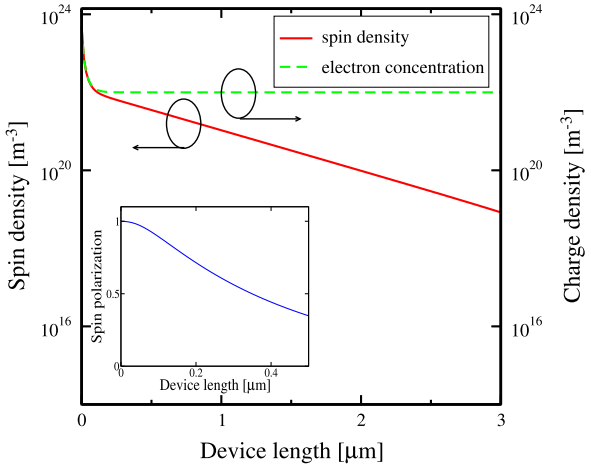

Fig. 7. Electron concentration and spin density distribution over the line under charge accumulation with the boundary as in (14), ($\mu_{Chem} = 100$ mV, $U_c = -300$ mV). The spin polarization (inset figure) is almost unchanged in the charge screening region. The charge current is 11.9 MA/m^2. The device length is 4 μm.

their values at the charge neutrality condition. This behavior is correlated with a significant increase of the minority spin current in the depletion layer, cf: Fig. 9. This current is due to two contributions, drift and diffusion, which add constructively in this case and cause the spin polarization to decrease substantially over a very short distance close to the interface. At the same time, the spin current density remains nearly constant through the depletion layer. Indeed, in this case the spin diffusion length is increased due to the high electric field at the depletion region. At the end of the space-charge layer the spin polarization is thus significantly smaller than the one at the interface explaining the spin current degradation in the bulk as compared to the one at the charge neutrality condition. We emphasize again that the sharp decrease of the spin polarization is due to the high spin minority current close to the interface. Should this current be reduced, for instance by applying a voltage of opposite polarity and inverting the current, cf Fig. 9, the spin current in the bulk is enhanced, but still remains below the level determined by the charge neutrality condition (Fig. 10).

Therefore, our results indicate that the spin injection through the space-charge layer and proper inclusion of screening does not result in a spin current enhancement in the bulk in comparison to the situation under the charge neutrality condition, when the space-charge layer is absent, provided the spin polarization at the interface and the charge currents are kept the same. Compared to [9] we have ignored here the effective magnetic field in the semiconductor generated by the injected spins. However, due to its smallness, it is unlikely that this field can drastically alter the results.

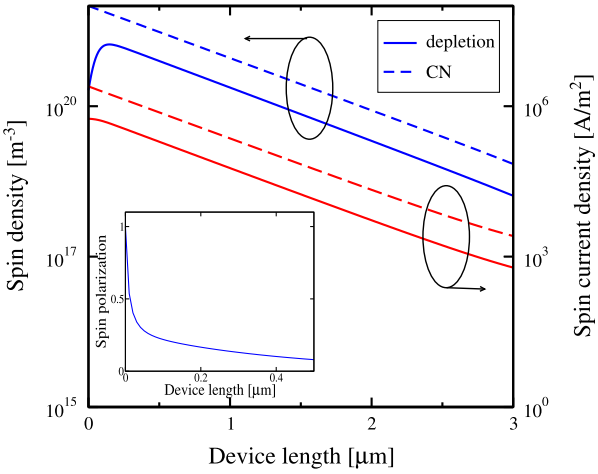

Fig. 8. Spin and spin current density in depletion ($\mu_{Chem} = -100$ mV, $U_c = -140.4$ mV) and the charge neutrality (*CN*) condition ($\mu_{Chem} = 0$ mV, $U_c = -204.1$ mV). The fixed charge current is 11.9 MA/m^2. The inset figure shows the spin polarization. The device length is 4 μm.

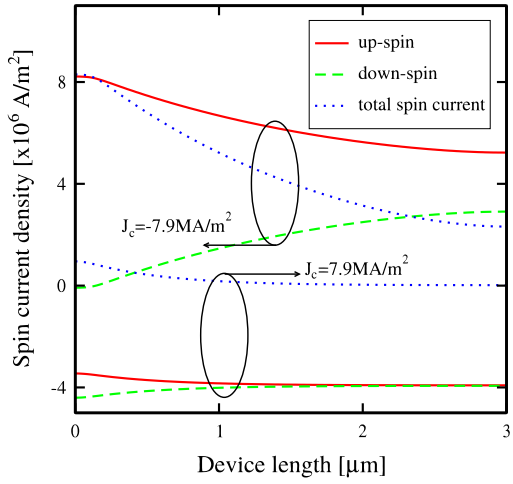

Fig. 9. Spin up (down) current densities and the total spin current density, when the device is in depletion. We keep $\mu_{Chem} = -100$ mV, with $U_c = 270$ mV for $J_c = -7.9$ MA/m^2 and $U_c = -24.6$ mV for $J_c = 7.9$ MA/m^2.

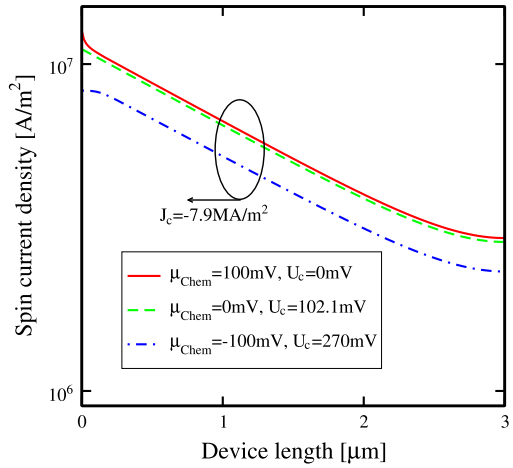

Fig. 10. Spin current density for accumulation, charge neutrality, and depletion with the boundary condition (14). The charge current is fixed at −7.9 MA/m^2.

4. Summary and conclusion

Spin injection in a semiconductor structure from a space-charge layer is considered. At a fixed interface spin polarization, the interface spin current is enhanced through injecting more charge, but is almost unchanged from that obtained at the charge neutrality condition in the bulk. In depletion the spin current in the bulk is suppressed. Thus, inclusion of the space-charge effects does not result in a higher spin injection efficiency as compared to the spin injection at the charge neutrality condition, when the spin polarization at the interface and the charge current are the same. Hence, at a fixed polarization, the charge neutrality determines the value of the maximum spin current possible provided the charge current is fixed. Accordingly, the largest spin current at charge neutrality is obtained at maximum spin polarization of the injected carriers, as intuitively expected.

Acknowledgment

This research is supported by the European Research Council through the Grant #247056 MOSILSPIN.

References

[1] Nikonov DE, Young IA. Overview of beyond-CMOS devices and a uniform methodology for their benchmarking. Computer 2013;36.
[2] Kim NS, Austin T, Baauw D, Mudge T, Flautner K, Hu JS, et al. Leakage current: moore's law meets static power. Computer 2003;36(December):68–75. http://dx.doi.org/10.1109/MC.2003.1250885.
[3] Jansen R. Silicon spintronics. Nat. Matter 2012;11(April):400. http://dx.doi.org/10.1038/nmat3293.
[4] Huang Biqin, Monsma Douwe J, Ian Appelbaum. Coherent spin transport through a 350 micron thick silicon wafer. Phys. Rev. Lett. 2007;99(October):177209. http://dx.doi.org/10.1103/PhysRevLett.99.177209.
[5] Sugahara S, Nitta J. Spin-transistor electronics: an overview and outlook. Proc IEEE 2010;98(October):2124–54. http://dx.doi.org/10.1109/JPROC.2010.2064272.
[6] Song Y, Dery H. Magnetic field modulated resonant tunneling in ferromagnetic-insulator-nonmagnetic junctions; 2014 [arXiv/1401.7649].
[7] [7] Txoperena O, Song Y, Qing L, Gobbi M, Hueso LE, Dery H, et al. Universal impurity-assisted tunneling magnetoresistance under weak magnetic field; 2014 [arxiv/1404.0633].
[8] van 't Erve OMJ, Friedman AL, Cobas E, Li CH, Robinson JT, Jonker BT. Low-resistance spin injection into silicon using graphene tunnel barriers. Nature Nano 2012;7:737.
[9] Sears MR, Saslow WM. Spin accumulation at ferromagnet/nonmagnetic material interfaces. Phys Rev B 2012;85(January):014404. http://dx.doi.org/10.1103/PhysRevB.85.014404.
[10] Zayets V. Spin and charge transport in materials with spin-dependent conductivity. Phys Rev B 2012;86(November):174415. http://dx.doi.org/10.1103/PhysRevB.86.174415.
[11] Yu ZG, Flatte ME. Spin diffusion and injection in semiconductor structures: electric field effects. Phys Rev B 2002;66(December):235302.
[12] Song Y, Dery H. Spin transport theory in ferromagnet/semiconductor systems with noncollinear magnetization configurations. Phys Rev B 2010;81:045321.
[13] Scharfetter D, Gummel H. Large-signal analysis of a silicon read diode oscillator. IEEE Trans Electron Dev 1969;16:64. http://dx.doi.org/10.1109/T-ED.1969.16566. ISSN 0018-9383.